Railton, CJ., Daniel, EM., Paul, DL., & McGeehan, JP. (1993). Optimized absorbing boundary conditions for the analysis of planar circuits using the finite difference time domain method. *IEEE Transactions on Microwave Theory and Techniques*, *41*(2), 290 - 297. https://doi.org/10.1109/22.216470

Optimized Absorbing Boundary Conditions for the Analysis of Planar Circuits Using the Finite Difference Time Domain Method

C. J. Railton, Elizabeth M. Daniel, Dominique-Lynda Paul, and Joseph P. McGeehan

Abstract— **The availability of effective numerical absorbing boundary conditions (ABCs) for use with the Finite Difference Time Domain (FDTD) method is essential for efficient application of the technique to microwave circuit analysis. Although many published results exist which have made use of various ABCs, little information concerning the optimum choice has been given. In this contribution, the suitability of available ABCs for planar circuit analysis is investigated and a new technique is presented whereby second order ABCs can be optimized for this type of problem.**

I. Introduction

THE FINITE DIFFERENCE TIME DOMAIN (FDTD) method is enjoying a considerable rise in popularity for the analysis of complex geometries such as microwave circuits. This is partly due to the increase both in the availability of computer power and the complexity of structures for which analysis is desired. The vast majority of problems to which FDTD is being applied involve open structures which, in turn, require the use of absorbing boundary conditions (ABCs) to correctly terminate the computational domain.

Over the last decades, a number of ABCs have been proposed and several are in common use. The ABCs most often referred to in the literature are those derived by Engquist and Majda [1] with the discretisation given by Mur [2]. These are based on approximating the outgoing wave equation by linear expressions using either a Taylor or Padé approximation. Recently this ABC has been extended for application to a nonuniform FDTD grid and to inhomogeneous material [3]. Other ABCs have been proposed by Higdon [4], Lindman [5] and Reynolds [6] but these appear to be less popular. An alternative approach has been followed by Fang and Mei [7] who use ABCs to estimate both the E and the H field at a point on the boundary and then combine the results in such a way as to improve the overall accuracy. Deveze et. al. also use a combination of the E and H field estimates in order to reduce the order of the derivatives which need to be evaluated [8]. Another technique, used mainly for scattering problems, includes estimating the angle of incidence of the wave by calculation of the Poynting vector [9].

Manuscript received March 20, 1992; revised March 12, 1992. This work was supported by the Science and Engineering Research Council and British Aerospace (Dynamics).

The authors are with the Centre for Communications Research, Faculty of Engineering, University of Bristol, BS8 1TR, England.

IEEE Log Number 9204486.

Although all of these ABCs have been used in conjunction with the FDTD method to produce results, little information has been given regarding the relative merits of the different techniques. The information which does exist, e.g. [10]–[12], is largely restricted to the behaviour of the ABCs with a single incident plane wave. In practice, this is a situation which never occurs. Little guidance exists, therefore, concerning how to choose the best ABC for a particular real problem. In this contribution, the behavior of some existing algorithms will be examined, for the more realistic case of a planar open waveguiding structure as well as for the case of plane wave incidence. A new technique will be presented whereby second order ABCs can be optimized for any given planar waveguiding structure and results will be given to verify the effectiveness of the method.

II. First and Second Order Absorbing Boundary Conditions

The first order approximation to the outgoing wave equation in the x direction is given by [1]:

$$(\partial_x - v^{-1}\partial_t)E = 0 \tag{1}$$

$$(\partial_x - v^{-1}\partial_t)H = 0 \tag{2}$$

where v is a parameter which can be freely chosen and corresponds to the assumed velocity of the incident wave normal to the boundary.

One form of the second order approximation is given as [1], [2]:

$$\partial_{tt}E_z = v\partial_{tx}E_z + kv^2(\partial_{zz}E_z + \partial_{yy}E_z) \tag{3}$$

where, in general, the parameters v and k can be freely chosen.

In [2], v is chosen to be equal to the speed of light in the material and k is chosen to be equal to 0.5. If k were chosen to be zero then (3) would reduce to the first order approximation for E. It can also be shown that if k were chosen as 1, then (3) would reduce to the first order approximation for H.

We can deduce the behavior of these ABCs to an incident plane wave in the following manner. Consider a plane wave with velocity c, travelling with an incident angle of ϑ to a boundary in the y-z plane. Without loss of generality we assume that the wave is polarized with E in the z direction.

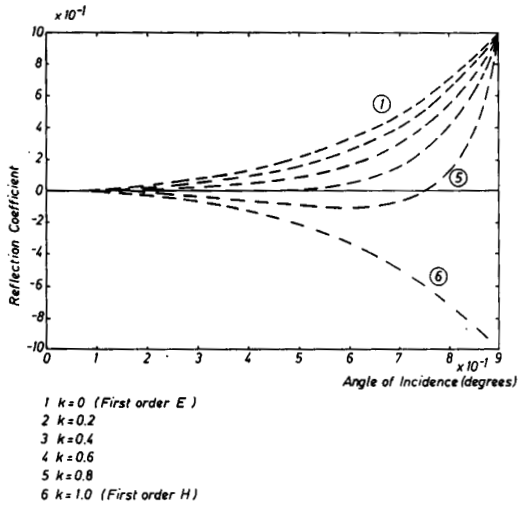

Fig. 1. Reflection coefficient versus angle of incidence for 2nd order ABCs.

Then:

$$E_z = F(x\,\mathrm{Cos}\,\vartheta + y\,\mathrm{Sin}\,\vartheta + ct)$$
$$\partial_{xx} = \mathrm{Cos}^2\,\vartheta \qquad \partial_{yy} = \mathrm{Sin}^2\,\vartheta$$
$$\partial_{xt} = c\,\mathrm{Cos}\,\vartheta \qquad \partial_{tt} = c^2$$

At the boundary there will be a reflection R which will cause the total field at the boundary to satisfy (3).

Therefore:

$$(1+R)c^2 - (1-R)vc\,\mathrm{Cos}\,\vartheta - (1+R)v^2k\,\mathrm{Sin}^2\,\vartheta = 0 \tag{4}$$

so

$$R = -\frac{c^2 - v^2k - vc\,\mathrm{Cos}\,\vartheta + v^2k\,\mathrm{Cos}^2\,\vartheta}{c^2 - v^2k + vc\,\mathrm{Cos}\,\vartheta + v^2k\,\mathrm{Cos}^2\,\vartheta} \tag{5}$$

Fig. 1 shows the way in which R varies as a function of ϑ and k for the case $v = c$. It can be seen that maximum flatness of the curve is found when $k \cong 0.65$. This would seem to be a better value than $k = 0.5$, as used in [2], if a wide spread in incident angle is expected.

If $k = 0.5$ and $v = c$ then:

$$R = \frac{(\mathrm{Cos}\,\vartheta - 1)^2}{(\mathrm{Cos}\,\vartheta + 1)^2} \tag{6}$$

If $k = 1$ and $v = c$ then we have:

$$R = \frac{(\mathrm{Cos}\,\vartheta - 1)}{(\mathrm{Cos}\,\vartheta + 1)} \tag{7}$$

corresponding to a first order magnetic ABC.

If $k = 0$ and $v = c$ then

$$R = -\frac{(\mathrm{Cos}\,\vartheta - 1)}{(\mathrm{Cos}\,\vartheta + 1)} \tag{8}$$

corresponding to a first order electric ABC.

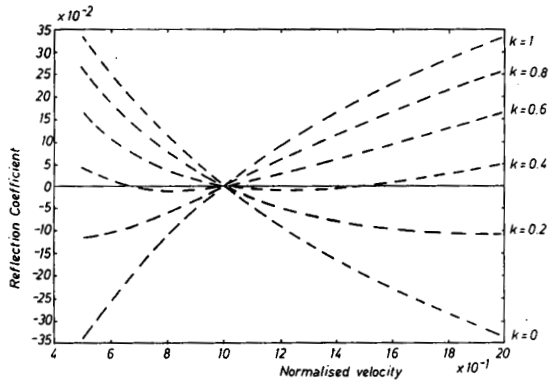

Fig. 2. Reflection coefficient versus velocity for 2nd order ABCs.

III. Behavior of Second Order ABC's for Waveguide Termination

The waves impinging on the boundaries of the computational domain surrounding a planar waveguide such as microstrip are not plane waves and, therefore, the above results are not directly applicable. In the direction of propagation, a waveguide, whether homogeneous or not, causes a wave to impinge normally on the boundary with some velocity, u, and some transverse variation, $f(y,z)$ which are, in general, functions of frequency. Fig. 2 shows the way in which the reflection coefficient, R, varies as a function of the normalized incident velocity.

For a general waveguiding structure, we may not know what the transverse variation, $f(y,z)$, is. It is, therefore, preferable to express (3) in an equivalent form which only involves the longitudinal derivatives. We can do this by using the wave equation:

$$(\partial_{yy} + \partial_{zz})E_z = (c^{-2}\partial_{tt} - \partial_{xx})E_z \tag{9}$$

where c is the speed of light in the material.

Substituting (9) into (3) we get:

$$\left\{\partial_{tt} - \frac{v}{1 - v^2k/c^2}\partial_{xt} + \frac{v^2k}{1 - v^2k/c^2}\partial_{xx}\right\}E_z = 0 \tag{10}$$

Now the E field as a function of space is given by:

$$E = f(y,z,x+ut) + Rf(y,z,x-ut) \tag{11}$$

where we assume a field of unit amplitude incident at the boundary and a reflected wave of amplitude R.

Therefore

$$\partial_{tt} = (1+R)u^2E$$
$$\partial_{tx} = (1-R)uE$$
$$\partial_{xx} = (1+R)E \tag{12}$$

To find the reflection coefficient, R, which causes the total field at the boundary to satisfy (10) we substitute as follows

$$(1+R)u^2 - (1-R)\frac{v}{1 - v^2k/c^2}u + (1+R)\frac{v^2k}{1 - v^2k/c^2} = 0 \tag{13}$$

therefore:

$$R = \frac{(1 - v^2k/c^2)u^2 - uv + kv^2}{(1 - v^2k/c^2)u^2 + uv + kv^2} \tag{14}$$

If v and c are chosen to be equal to the velocity of propagation, then $R = 0$ regardless of the choice of k. For a dispersive waveguide, v and k can be chosen to minimize the total reflection.

IV. Optimizing the ABC's for an Inhomogeneous Waveguide

Although the method described above can yield very low total reflected power, it is not ideal for the case of an inhomogeneous waveguide because the local value of R varies across the cross-section of the boundary. This leads to the excitation of higher order modes which may cause inaccuracies in the final result, especially if the incident pulse contains frequency components at which these higher order modes can propagate. A better technique is to choose values of v and k separately for each dielectric region. Given that we wish to minimize the returned energy from a broad band pulse which has a frequency range of interest $\{f\}$, and hence a velocity range of interest $\{u\}$, we can choose the best values of the parameters v and k in the following manner:

For convenience, we make the following assignments:

$$u = \frac{c_0}{\sqrt{\epsilon_{\text{eff}}}}, \qquad c = \frac{c_0}{\sqrt{\epsilon_r}}, \qquad v = \frac{c_0}{\sqrt{\epsilon_b}},$$

where

ϵ_{eff} is the effective permittivity of the waveguide.

ϵ_r is the permittivity of the dielectric layer under consideration.

ϵ_b is determined from the choice of the parameter v.

We can then find the average reflected power for a given v and k by evaluating the integral over the effective permittivity of interest. $w(\epsilon_{\text{eff}})$ represents the approximate spectrum of the incident pulse.

$$\frac{\int w(\epsilon_{\text{eff}})\, R(v, k, \epsilon_{\text{eff}})\, d\epsilon_{\text{eff}}}{\int w(\epsilon_{\text{eff}})\, d\epsilon_{\text{eff}}} \tag{15}$$

The values of v and k which minimize this expression are the optimum values for the problem under consideration.

For the microstrip line having the geometry shown in Fig. 3 and a frequency range of interest of 1–10 GHz, the range of effective permittivity is approximately $5.9 - 7$. Fig. 4 shows the value of (15) for $5.9 < \epsilon_{\text{eff}} < 7$, and dielectric permittivity of 8.875. $w(\epsilon_{\text{eff}})$ is taken as unity. It can be shown that, in order to minimize (15), we should choose $k = 0.65, \epsilon_b = 9.3$. Similarly, for the air region we should choose $k = 0.3, \epsilon_b = 1.7$. The expression (15) is only weakly dependent on the range of effective permittivity and, therefore, available closed form approximations, e.g. [13], are entirely adequate to calculate them. Moreover, the calculation of the optimum parameters requires very little computational effort and is easily included in the setting up stage of the FDTD algorithm.

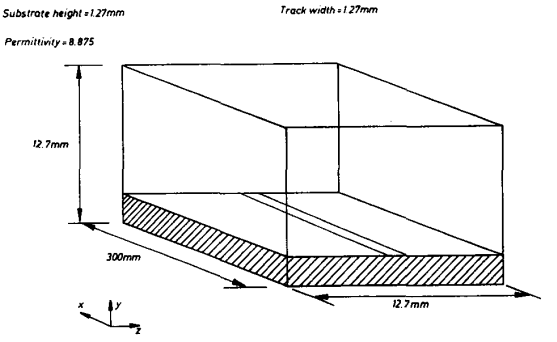

Fig. 3. Microstrip geometry used for comparisons.

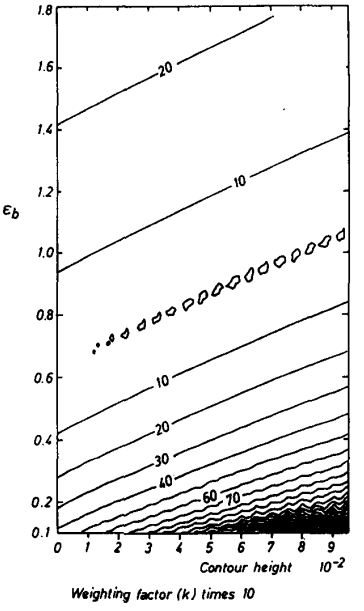

Fig. 4. Reflection coefficient in microstrip substrate of 2nd order ABCs versus weighting factor (k) and ϵ_b.

V. Discretization of the Second Order ABC's

Although the discretization given by Mur [2] for the second order boundary condition is widely used, an alternative discretization which is more convenient to implement will be developed. This has some similarity to the "super-absorbing" ABC [7]. We use the discretization for the first order absorbing boundary conditions given in [2] in order to estimate the tangential E and H fields outside the boundary. The estimated value of H, together with the FDTD discretization of Maxwell's equations is then used to produce a second estimate of the tangential E field and a weighted average of the two estimates is used. The difference of our approach to that of [7] is that the parameters, k and ϵ_b, are calculated separately for each dielectric layer and each dielectric interface. That this

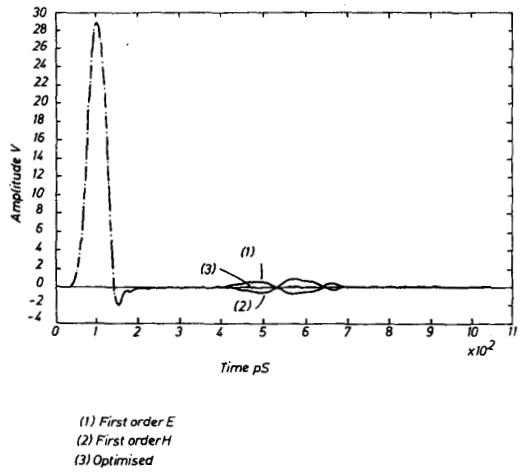

Fig. 5. Reflection from various ABCs of a broad band pulse on microstrip.

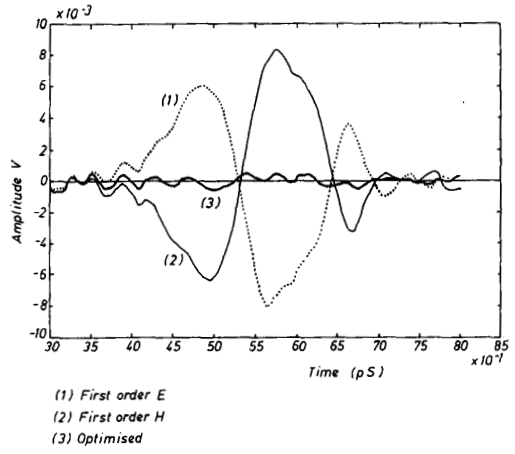

Fig. 6. Expanded view of reflected pulse using different ABCs.

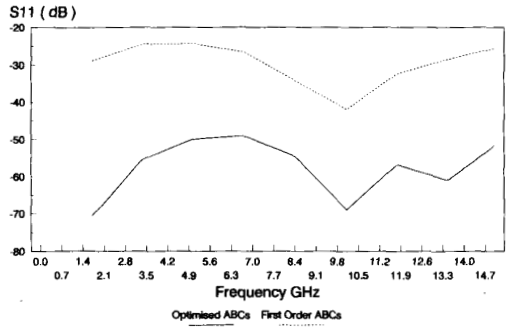

Fig. 7. Reflection coefficient of ABCs versus Frequency.

discretization scheme represents the same differential equation (3) is shown in the Appendix.

The optimization of the ABCs at the dielectric interface is carried out in the following manner. On the $+x$ face of the problem space we require to estimate the value of E_z on the dielectric interface which is assumed to be in the x-y plane. In this case the value of ϵ used in (18) must be the weighted average of the permittivities above and below the interface as given in [14]. Thus the value of ϵ_r used when evaluating the integral (15) is given by:

$$\frac{dz_1\epsilon_1 + dz_2\epsilon_2}{dz_1 + dz_2}$$

where dz_1 and dz_2 is the grid spacing in the direction normal to the dielectric/air interface in the dielectric and air regions respectively and ϵ_1 and ϵ_2 are the permittivities in the dielectric and air regions, respectively.

The value of (15) for the case of $\epsilon = 4.9375$, i.e. the average of 1 and 8.875 corresponding to $dz_1 = dz_2$ is a minimum if we choose $k = 0.45$ and $\epsilon_b = 5$.

VI. Results for Microstrip Structures

Initial tests were carried out on a uniform microstrip line with dimensions given in Fig. 3 and using a non-uniform grid consisting of $36 \times 24 \times 40$ unit cells. Fig. 5 shows the reflected pulse from first order electric and magnetic ABCs and the reflection from a optimized absorbing ABC with parameters extracted from minimizing (15), viz. In the air region, $\epsilon_b = 1.7, k = 0.3$. In the substrate, $\epsilon_b = 9.3, k = 0.65$. At the air/dielectric interface $\epsilon_b = 5, k = 0.45$. On the scale of Fig. 5 the reflection from the optimized ABC is too small to be seen. An expanded view of the reflection, Fig. 6 reveals that the peak amplitude of the reflected pulse is approximately ± 0.0008 V which is 0.3% of the height of the incident pulse and is comparable to the numerical noise in the mesh. This is approximately 20 dB better than the first order ABCs. The performance of the ABCs in the frequency domain is shown in Fig. 7 where the reflection coefficients are plotted as a function of frequency.

The effect of imperfect absorbing boundary conditions has the greatest impact on problems such as the calculation of the dispersion characteristic of a transmission line where the relative phase of the propagating wave is required. Fig. 8 shows the calculated dispersion curve for the microstrip whose geometry is given in Fig. 3 for different absorbing boundaries. For comparison, the same test was carried out using a line long enough so that the reflection could be eliminated from the calculation. It can be seen that the optimized ABC, although giving rise to a noticeable ripple on the curve, is greatly superior to the first order Mur ABC.

VII. Effect of Imperfect ABCs on Characterization of Complex Circuits

In order to assess the effect of ABC imperfections of the calculated S parameters of components of more realistic complexity, tests were carried on a low pass filter previously modelled in [15] and [16], a band-pass side coupled filter modelled in [17] and [16], and a spiral inductor previously modelled in [18]. Each of these structures were modelled using a non-uniform grid.

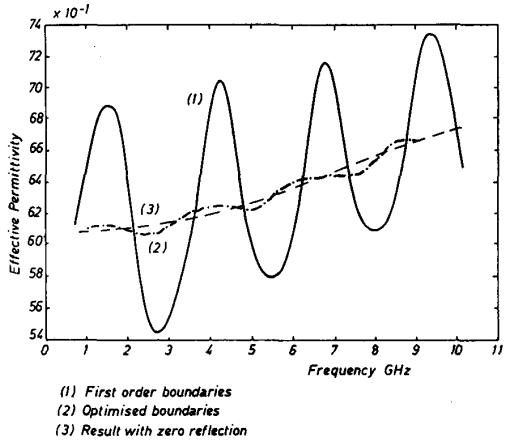

Fig. 8. Calculated microstrip dispersion characteristics using various ABCs.

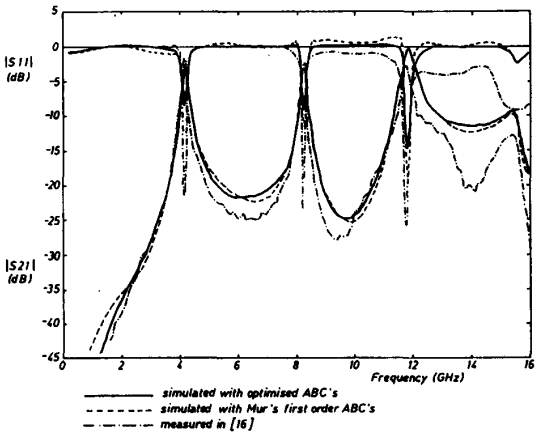

Fig. 10. Scattering parameters of the side-coupled filter.

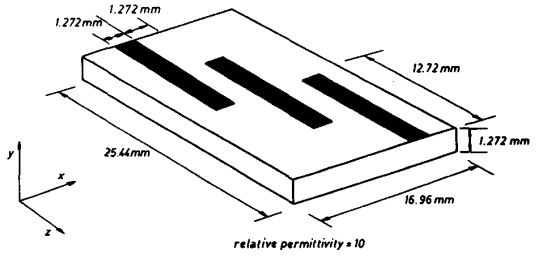

Fig. 9. Side coupled filter detail.

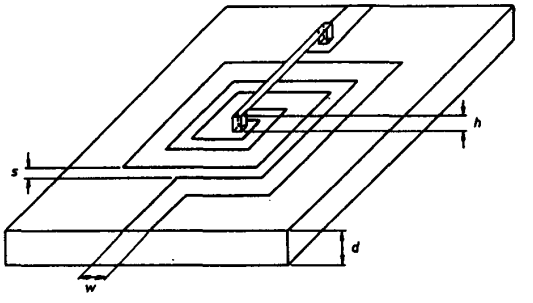

Fig. 11. Geometry of a spiral inductor.

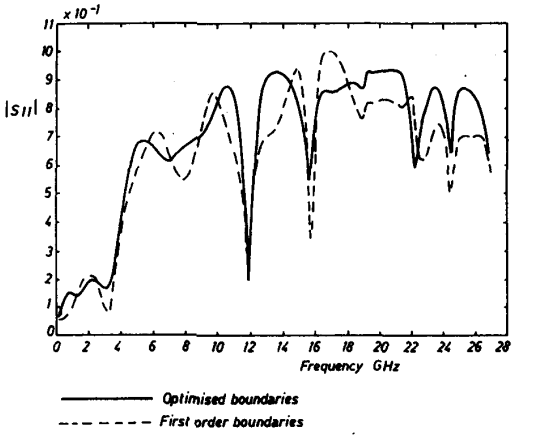

Fig. 12. Reflection coefficient of the spiral inductor.

For the case of the low-pass filter, it was found that the results obtained from using the optimized ABCs were not significantly different from those obtained using the first order ABCs.

The results for the bandpass filter whose geometry is given in Fig. 9 are shown in Fig. 10 for various ABCs. Here it can be seen that, although there is little difference between the results, those obtained using the optimized ABCs are better in the case of S_{11} and comparible in the case of S_{21}. For this filter a non-uniform grid consisting of $68 \times 16 \times 72$ unit cells was used.

Results for the case of the spiral inductor, [18], whose geometry is shown in Fig. 11 are given in Fig. 12. Here it can be seen that there is considerable ripple on the results obtained using the first order ABCs which has largely been eliminated by the use of the optimized ABCs. In particular, the peak in S_{11} at 17 GHz is calculated to be greater than unity with the first order ABCs. The results from the optimized ABCs are in much better agreement with the measurements presented in [18]. A nonuniform grid consisting of $60 \times 14 \times 86$ cells was used in this simulation.

From the foregoing it can be concluded that, although for circuits and components whose behavior is largely governed by resonant effects the choice of ABCs is not critical. In this category would come resonators, filters etc. For circuits whose behavior is largely governed by the phase changes produced by transmission lines the optimized ABCs yields considerable improvement. In the latter category would come transitions, junctions, couplers etc. For this important group of components the use of optimized ABCs is highly desirable.

VIII. Boundaries Transverse to the Direction of Propagation

Once a waveguide mode is established, the wave impinges on the boundaries transverse to the direction of propagation

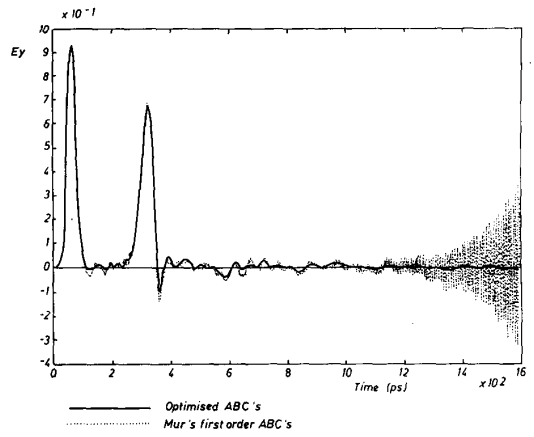

Fig. 13. Transient response on the input port when the ABCs are placed at a position of strong electromagnetic field.

($\pm x$ and $+y$ for the geometry of Fig. 9) at an angle of 90°. It can be seen from Fig. 1 that the second order ABCs will give a reflection coefficient of unity regardless of the values of the parameters when a single plane wave impinges with this angle of incidence. The situation is, in fact, exascerbated by the fact that the velocity of propagation is not equal to c. This is equivalent to the sum of plane waves entering and *emerging from* the boundary with an angle of $\mathrm{Sin}^{-1}(u/c)$. Since $R > 1$ for the latter case, we have a potentially unstable situation. In practice this means that for long time periods or for boundaries which are placed where the field strength is high, instability is likely to be observed. This phenomenon has also been observed in [19]. The effect is illustrated in Fig. 13 which shows the time response of the structure of Fig. 9 where the boundaries have been placed close to the metal strip. It can be seen that instability appears in the late time response. The effect can be mitigated but not removed by the use of the second order ABCs. It has been found that if the time sequence is truncated too close to the point where instability occurs, the calculated frequency domain results are inaccurate. An investigation into the factors which influence the onset of instability have shown the following:

1) The size of the unit cells adjacent to the boundaries have little effect on the stability of the ABC.
2) The ABCs were found to be stable if a metal boundary is used for the $+y$ face but potentially unstable otherwise.
3) The choice of the parameters v and k affect the time before the onset of instability but do not prevent it entirely.
4) Introducing loss in the mesh close to the $+y$ boundary caused only a marginal improvement in stability.
5) The only parameter which was found to affect the stability of the ABCs strongly is the height of the $+y$ face above the substrate. For the geometry of Fig. 9, this effect is shown in Table I. Here it can be seen that changing the box height from 1.5 h to 2.5 h stopped the onset on instability during the observation time whereas changing the type of ABC made at most a 50% improvement. In addition it was found that the accuracy of the final result was adversely affected if the box height was less than about 3 h.
6) If the box height was set to 4 h then the effect of changing the $+y$ face from an ABC to a metal boundary was very small.

TABLE I
EFFECT OF BOX HEIGHT ON ABC STABILITY FOR THE STRUCTURE OF FIG. 8

H/h	T_1	T_2
1.5	1.2 nS	1.8 nS
2.0	5.0 nS	> 6.0 nS
2.5	> 6.0 nS	> 6.0 nS

H is the height of the +y boundary
h is the height of the substrate
T_1 is the time before the first order ABCs become unstable
T_2 is the time before the optimized ABCs become unstable

From this we can conclude that, for any of the ABCs considered, the $+y$ face must be placed at a height of 3 h or more above the substrate in order to achieve stability. Since, at this height the field strength is low, the use of a metal wall has little effect on the overall result. It is expected, therefore that the most effective scheme is to use optimized boundaries on the $+z$ and $+x$ faces, and to use a metal wall on the $+y$ face.

It is noted that the problem of instability will be most apparent for a structure such as Fig. 9 since, by its highly resonant nature, a long time sequence is required. For the simpler structure of Fig. 3, the required time sequence is likely to be short enough so that no instability will be observed.

IX. CONCLUSIONS

In this contribution it has been shown that the description of absorbing boundary condition algorithms in terms of single incident plane waves is not sufficient information from which to choose the best ABC for planar waveguide termination. A new technique has been demonstrated whereby the ABCs can be optimized which results in a return loss from a wideband pulse less than -50 dB. Moreover this technique reduces the risk of loss of accuracy due to mode conversion taking place at the boundary. The use of these optimized ABCs causes considerable improvement in the results of analyses of an important category of microstrip components. For boundaries transverse to the direction of propagation, we have shown that inaccuracy and late time instability can result if the boundary is placed in regions of high field strength.

APPENDIX
DISCRETIZATION OF SECOND ORDER ABCS

We consider a boundary situated in the y-z plane. At the start of the iteration we assume that we have E^{n+1} and $H^{n+1/2}$ at all points except the boundary plane and E^n and $H^{n-1/2}$ at all points including the boundary plane. We form our first estimate of E_z at time $n+1$ in the boundary as follows:

$$E_z^{n+1}(0,j,k+1/2) = E_z^n(1,j,k+1/2) + K_1\big(E_z^{n+1}(1,j,k+1/2) - E_z^n(0,j,k+1/2)\big) \quad \text{(A1)}$$

The second estimate of E_z makes use of the standard FDTD formula:

$$\begin{aligned} E_z^{n+1}(0,j,k+1/2) = E_z^n(0,j,k+1/2) \\ + K_2\big(H_x^{n+1/2}(0,j+1/2,k+1/2) \\ - H_x^{n+1/2}(0,j-1/2,k+1/2)\big) \\ + K_3\big(H_y^{n+1/2}(1/2,j,k+1/2) \\ - H_y^{n+1/2}(-1/2,j,k+1/2)\big) \end{aligned} \quad \text{(A2)}$$

where the K's are constants involving the mesh size and the material properties.

Combining (A2) with the similar equation used for the previous iteration we get:

$$\begin{aligned} E_z^{n+1}(0,j,k+1/2) - 2E_z^n(0,j,k+1/2) \\ + E_z^{n-1}(0,j,k+1/2) \\ = K_2\big(H_x^{n+1/2}(0,j+1/2,k+1/2) \\ - H_x^{n+1/2}(0,j-1/2,k+1/2)\big) \\ - K_2\big(H_x^{n-1/2}(0,j+1/2,k+1/2) \\ - H_x^{n-1/2}(0,j-1/2,k+1/2)\big) \\ + K_3\big(H_y^{n+1/2}(1/2,j,k+1/2) \\ - H_y^{n+1/2}(-1/2,j,k+1/2)\big) \\ - K_3\big(H_y^{n-1/2}(1/2,j,k+1/2) \\ - H_y^{n-1/2}(-1/2,j,k+1/2)\big) \end{aligned} \quad \text{(A3)}$$

The values of $H_x^{n+1/2}$ on the boundary can be derived from the values of E_y^{n-1} and E_z^{n-1} calculated on the previous iteration. The values of $H_y^{n-1/2}$ on the boundary are calculated using Mur's discretization of the first order absorbing boundary condition:

$$\begin{aligned} H_y^{n+1/2}(-1/2,j,k+1/2) = H_y^{n-1/2}(1/2,j,k+1/2) \\ + K_4\big(H_y^{n+1/2}(1/2,j,k+1/2) \\ - H_y^{n-1/2}(-1/2,j,k+1/2)\big). \end{aligned} \quad \text{(A4)}$$

Substituting equation (A4) into (A3) we get:

$$\begin{aligned} E_z^{n+1}(0,j,k+1/2) - 2E_z^n(0,j,k+1/2) \\ + E_z^{n-1}(0,j,k+1/2) \\ = K_2K_6\big(E_z^{n+1}(0,j+1,k+1/2) \\ - E_z^{n+1}(0,j,k+1/2)\big) \\ + K_2K_7\big(E_y^{n+1}(0,j+1/2,k+1) \\ - E_y^{n+1}(0,j+1/2,k)\big) \\ + K_2K_6\big(E_z^{n-1}(0,j+1,k+1/2) \\ - E_z^{n-1}(0,j,k+1/2)\big) \\ + K_2K_7\big(E_y^{n-1}(0,j+1/2,k+1) \\ - E_y^{n-1}(0,j+1/2,k)\big) \\ + K_3\big(H_y^{n+1/2}(1/2,j,k+1/2) \\ + H_y^{n-1/2}(1/2,j,k+1/2)\big) \\ + K_3\big(H_y^{n-1/2}(-1/2,j,k+1/2) \\ + H_y^{n-3/2}(-1/2,j,k+1/2)\big) \\ + K_3K_1\big(H_y^{n+1/2}(1/2,j,k+1/2) \\ - H_y^{n-1/2}(-1/2,j,k+1/2)\big) \\ + K_3K_1\big(H_y^{n-1/2}(1/2,j,k+1/2) \\ - H_y^{n-3/2}(-1/2,j,k+1/2)\big). \end{aligned} \quad \text{(A5)}$$

We can now express both estimates of $E_z^{n+1}(0,j,k+1/2)$ in terms of the quantities known at the start of the iteration.

We now show the correspondence of this scheme with the second order differential equation (3).

In the limit of small time and space increments, equation (A5) becomes:

$$\partial_{tt}E_z = \frac{1}{\epsilon}\Big(v^{-1}(\partial_{tt}H_y) - \mu^{-1}(\partial_{zy}E_y - \partial_{yy}E_z)\Big) \quad \text{(A6)}$$

We can replace $\partial_t H_y$ using the FDTD formula to derive an equation involving only the electric field:

$$\begin{aligned} \partial_{tt}E_z &= \frac{1}{\epsilon\mu}\left(\frac{1}{v}(\partial_{tx}E_z - \partial_{tz}E_x) - (\partial_{zy}E_y - \partial_{yy}E_z)\right) \\ &= \frac{c^2}{v}(\partial_{tx}E_z - \partial_{tz}E_x) - c^2(\partial_{zy}E_y - \partial_{yy}E_z) \end{aligned} \quad \text{(A7)}$$

where $c = 1/\sqrt{\epsilon\mu}$ is the speed of light in the dielectric material. This gives us our second estimate of E_z.

The first estimate, given by (1), upon differentiation leads to:

$$\partial_{tt}E_z = v\partial_{tx}E_z. \quad \text{(A8)}$$

If we take a weighted average of the expressions (A8) and (A7) we get:

$$\begin{aligned} \partial_{tt}E_z = \left(\frac{c^2}{v}k + (1-k)v\right)\partial_{tx}E_z - \frac{c^2}{v}k\partial_{tz}E_x \\ - kc^2(\partial_{zy}E_y - \partial_{yy}E_z) \end{aligned} \quad \text{(A9)}$$

Using the fact that $\nabla \cdot \boldsymbol{E} = 0$ and that, from (1)

$$\partial_{tz}E_x = v\partial_{xz}E_x. \quad \text{(A10)}$$

we can write equation (A9) as follows:

$$\partial_{tt}E_z = \left(\frac{c^2}{v}k + (1-k)v\right)\partial_{tx}E_z + kc^2(\partial_{zz}E_z + \partial_{yy}E_z) \quad \text{(A11)}$$

If $k = 0.5$ and $v = c$ then this is the same as Mur's second order condition.

REFERENCES

[1] B. Engquist and A. Majda, "Absorbing boundary conditions for the numerical simulation of waves," *Math. Comp.*, vol. 31, pp. 629–651, July 1977.

[2] G. Mur, "Absorbing boundary conditions for the finite difference approximation of the time-domain electromagnetic-field equations," *IEEE Trans. Electromagn. Compat.*, vol. 23, pp. 377–382, Nov. 1981.

[3] E. M. Daniel and C. J. Railton, "An improved second order radiating boundary condition for use with non-uniform grids in the finite difference time domain method," in *Proc. 21st EuMC*, Stuttgart, Sept. 1991, pp. 547–552.

[4] R. L. Higdon, "Numerical absorbing boundary conditions for the wave equation," *Math. Comp.*, vol. 49, pp. 65–91, July 1987.

[5] E. L. Lindman, "Free space boundary conditions for the time dependent wave equations," *J. Comp. Phys.*, vol. 18, pp. 66–78, 1975.

[6] A. C. Reynolds, "Boundary conditions for the numerical solution of wave propagation problems," *J. Phys.*, vol. 43, no. 6, pp. 1099–1110, Oct. 1978.
[7] J. Fang and K. K. Mei, "A super-absorbing boundary algorithm for solving electromagnetic problems by the time domain finite difference method," in *IEEE AP-S Symp. Dig.*, 1988, pp. 472–475.
[8] T. Deveze, F. Clerc, and W. Tabbara, "Second order pseudo-transparent boundary equations for FDTD method," in *IEEE AP-S Symp. Dig.*, 1990, pp. 1624–1627.
[9] C. L. Britt, "Solution of electromagnetic scattering problems using time domain techniques," *IEEE Trans. Microwave Theory Tech.*, vol. 37, pp. 1181–1192, Sept. 1989.
[10] F. X. Canning, "On the application of some radiation boundary conditions," *IEEE Trans. Antennas Propagat.*, vol. 38, pp. 740–745, May 1990.
[11] T. G. Moore, J. G. Blaschlak, A. Taflove, and G. A. Kriegsmann, "Theory and application of radiation boundary operators," *IEEE Trans. Antennas Propagat.*, vol. 36, pp. 1797–1812, Dec. 1988.
[12] J. G. Blaschak and G. A. Kriegsmann, "A comparitive study of absorbing boundary conditions," *J. Comp. Phys.*, vol. 77, pp. 109–139, July 1988.
[13] M. Kirsching and R. H. Jansen, "Accurate model for effective dielectric constant of microstrip with validity up to millimetre wave frequencies," *Electron. Lett.*, vol. 18, pp. 272–273, 1982.
[14] C. J. Railton and J. P. McGeehan, "An analysis of microstrip with rectangular and trapezoidal conductor cross-section," *IEEE Trans. Microwave Theory Tech.*, vol. 38, pp. 1017–1022, Aug. 1990.
[15] D. M. Sheen, S. M. Ali, M. D. Abouzahra, and J. A. Kong, "Application of the three-dimensional finite-difference time-domain method to the analysis of planar microstrip circuits," *IEEE Trans. Microwave Theory Tech.*, vol. 38, pp. 849–857, July 1990.
[16] D. L. Paul, E. M. Daniel, and C. J. Railton, "Fast finite difference time domain method for the analysis of planar microstrip circuits," in *Proc. 21st EuMC*, Stuttgart, 1991, pp. 303–308.
[17] T. Shibata, T. Hayashi, and T. Kimura, "Analysis of microstrip circuits using three-dimensional full-wave electromagnetic field analysis in the time domain," *IEEE Trans. Microwave Theory Tech.*, vol. MTT-29, pp. 1064–1070, June 1988.
[18] M. Rittweger and I. Wolff, "Analysis of complex passive (M)MIC components using the finite difference time domain approach," in *IEEE MTT-S Int. Microwave Symp. Dig.*, Dallas, 1990, pp. 1147–1150.
[19] P. D. Smith and S. R. Cloude, "Time domain modelling: Integral equations, finite differences and experimental results," in *Proc. Inst. Elec. Eng. Conf. on Computation in Electromagnetics*, London, 1991.

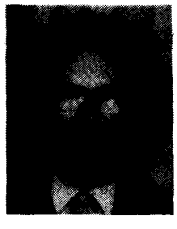

C. J. Railton received the BSc degree (with honors) in physics with electronics from the University of London in 1974 and the Ph.D. degree in electronic engineering from the University of Bath in 1988.

During the period 1974–1984 he worked in the scientific civil service on a number of research and development projects in the areas of communications and signal processing. Between 1984 and 1987 he worked at the University of Bath on the mathematical modelling of boxed microstrip circuits. Dr. Railton currently works in the Centre for Communications Research at the University of Bristol where he leads a group involved in the mathematical modelling and the development of CAD tools for MMICs, antennas, microwave heating systems, EMC and high-speed logic.

Elizabeth M. Daniel was born in 1967 in Worcestershire, England. In 1989, she received the B.Eng. degree (with honors) in electrical and electronic engineering from the University of Bristol. She is currently pursuing the PhD. degree at the Centre of Communications Research, University of Bristol. Her current research interests include the development of the Finite Difference Time Domain method for the modelling of planar antennas, especially radiating boundary conditions.

Dominique-Lynda Paul was born in Blida, Algeria, on January 16, 1961. She received the D.E.A. degree in electronics from Brest University in June 1986 and the Ph.D. degree from "Ecole Nationale Supérieure des Télécommunications de Bretagne" (LEST-ENSTBr) in January 1990.

She is now working as a post-doctoral research associate at the Communications Research Centre, University of Bristol. Her research interests include the modelling of passive planar microstrip devices and the characterization of dielectric systems at millimeter wavelengths.

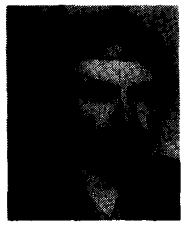

Joseph P. McGeehan obtained the degrees of B.Eng. (Hons) and Ph.D. in electrical and electronic engineering from the University of Liverpool, England in 1967 and 1971, respectively.

From 1970 to 1972 he held the position of senior scientist at the Allen Clarke Research Centre, The Plessey Company Ltd., where he was primarily responsible for the research and development of high-power millimeter-wave devices (two- and three-terminal) for ultra-high-speed logic. In September 1972 he was appointed to the academic staff of the University of Bath, England, where he led research groups in mobile communications, signal processing and microwave techniques. Since July 1985 he has held the chair of Communications Engineering in the Department of Electrical and Electronic Engineering, University of Bristol, England, and is director of the Centre for Communications Research there.

Dr. McGeehan is a member of a number of national and international committees in the field of communications.